Strongly correlated systems in atomic and condensed matter physics

Lecture notes

by Eugene Demler

ETH

October 18, 2023

Chapter 6

Topological properties of Bloch bands

6.1 Su-Schrieffer-Heeger model

In this section we will discuss the famous Su-Schrieffer-Heeger (SSH) model of particles hopping on a 1d tight-binding lattice that has two kinds of bonds [1]

$$\mathcal{H}_{\text{SSH}} = -t_1 \sum_n (c^\dagger_{nA} c_{nB} + c^\dagger_{nB} c_{nA}) - t_2 \sum_n (c^\dagger_{nB} c_{n+1A} + c^\dagger_{n+1A} c_{nB}) \tag{6.1}$$

There are two atoms in every unit cell, which we denote as A and B (see fig. 6.1), hence we expect to find two bands. For now we will assume that the system has periodic boundary conditions.

We perform Fourier transforms of creation/annihilation operators

$$\begin{pmatrix} c_{nA} \\ c_{nB} \end{pmatrix} = \frac{1}{\sqrt{N}} \sum_n e^{-ikn} \begin{pmatrix} c_{kA} \\ c_{kB} \end{pmatrix} \tag{6.2}$$

where N is the total number of sites. We can now write the Hamiltonian (6.1) as

$$\mathcal{H}_{\text{SSH}} = \sum_k (c^\dagger_{kA} c^\dagger_{kB}) \begin{pmatrix} 0 & -t_1 - t_2 e^{ik} \\ -t_1 - t_2 e^{-ik} & 0 \end{pmatrix} \begin{pmatrix} c_{kA} \\ c_{kB} \end{pmatrix} \tag{6.3}$$

Note that in writing (6.3) we took the size of the unit cell (distance between two A sites) to be equal to one.

We use the method of operator equations of motion to find eigenenergies and eigenstates. Let us assume that the Hamiltonain (6.3) can be diagonalized using operators $\gamma_{k,\lambda}$, so that

$$\mathcal{H}_{\text{SSH}} = \sum_{k,\lambda} \epsilon_{k,\lambda} \gamma^\dagger_{k,\lambda} \gamma_{k,\lambda} \tag{6.4}$$

$$\gamma^\dagger_{k,\lambda} = \psi_{Ak,\lambda} c^\dagger_{k,A} + \psi_{Bk,\lambda} c^\dagger_{k,B} \tag{6.5}$$

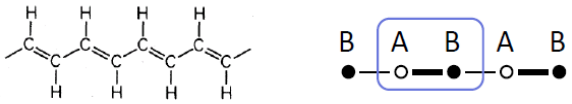

Figure 6.1: SSH model

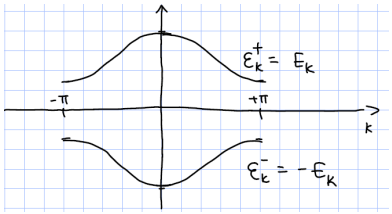

Figure 6.2: Band structure of the SSH Hamiltonian (6.1).

From equation (6.4) we have

$$[H, \gamma^\dagger_{k,\lambda}] = \epsilon_{k,\lambda}\gamma^\dagger_{k,\lambda} \tag{6.6}$$

On the other hand, we can use (6.5) and anticommutation relations of $c_{k,A/B}$ operators to find

$$\begin{aligned}[H, \gamma^\dagger_{k,\lambda}] &= \psi_{Ak,\lambda}c^\dagger_{k,B}(-t_1 - t_2 e^{-ik}) + \psi_{Bk,\lambda}c^\dagger_{k,A}(-t_1 - t_2 e^{ik}) \\ &= \epsilon_{k,\lambda}\gamma^\dagger_{k,\lambda} = \epsilon_{k,\lambda}(\psi_{Ak,\lambda}c^\dagger_{k,A} + \psi_{Bk,\lambda}c^\dagger_{k,B})\end{aligned} \tag{6.7}$$

From (6.7) we find

$$\epsilon_{k,\lambda}\begin{pmatrix}\psi_{Ak,\lambda}\\ \psi_{Bk,\lambda}\end{pmatrix} = -\begin{pmatrix}0 & t_1 + t_2 e^{ik}\\ t_1 + t_2 e^{-ik} & 0\end{pmatrix}\cdot\begin{pmatrix}\psi_{Ak,\lambda}\\ \psi_{Bk,\lambda}\end{pmatrix} \tag{6.8}$$

This looks like equation for a spin $\frac{1}{2}$ particle in magnetic field. We find eigenenergies

$$\epsilon_{k,\pm} = \pm E_k \tag{6.9}$$

$$E_k = \sqrt{(t_1 + t_2\cos k)^2 + (t_2 \sin k)^2} \tag{6.10}$$

The band structure is shown in fig.6.2.

To find eigenstates it is convenient to write $t_1 + t_2 e^{ik} = e^{i\frac{k}{2}}(t_1 e^{-i\frac{k}{2}} + t_2 e^{i\frac{k}{2}}) = E_k e^{i\frac{k}{2} + i\theta_k}$ where

$$\tan\theta_k = \frac{(t_2 - t_1)\sin\frac{k}{2}}{(t_1 + t_2)\cos\frac{k}{2}} \tag{6.11}$$

and we find

$$\begin{pmatrix}\Psi_{Ak,-}\\ \psi_{Bk,-}\end{pmatrix} = \frac{1}{\sqrt{2}}\begin{pmatrix}1\\ e^{-i\frac{k}{2} - i\theta_k}\end{pmatrix} \qquad \begin{pmatrix}\psi_{Ak,+}\\ \psi_{Bk,+}\end{pmatrix} = \frac{1}{\sqrt{2}}\begin{pmatrix}-1\\ e^{-i\frac{k}{2} - i\theta_k}\end{pmatrix} \tag{6.12}$$

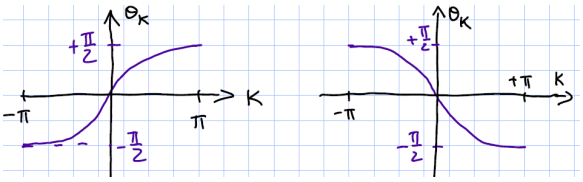

Figure 6.3: Winding of θ_k from eq. 6.11. Figure on the left corresponds to $t_2 > t_1$ and figure on the right to $t_2 < t_1$.

Note the difference in the behavior of θ_k across the Brillouin zone depending on which t_1 or t_2 is larger (see fig. 6.3).

To understand the topological character of the SSH model it is convenient to represent the Hamiltonian (6.3) as

$$\mathcal{H}_{\rm SSH} = \sum_{k\alpha\beta} \vec{d}(k)\vec{\sigma}_{\alpha\beta} c^\dagger_{\alpha k} c_{\beta k} \tag{6.13}$$

$$d_x(k) = -t_1 - t_2\cos k \qquad\qquad d_y(k) = t_2 \sin k \tag{6.14}$$

Here α and β represent sublattice indices A and B. Vector $\vec{d}(k)$ should be in the XY plane since the hamiltonian only has terms connecting A and B sublattices. Consider evolution of this vector as we change momentum through the Brillouin zone between $-\pi$ and π. The two regimes $t_1 > t_2$ and vice versa correspond to two topologically distinct trajectories: one encircles the origin and the other does not. The two can not be smoothly connected without either closing the gap or changing the symmetry of the hamiltonian. If the $\vec{d}(k)$ stays in the plane but goes through the origin, it corresponds to the case $t_1 = t_2$, when the gap between the bans closes. If we try to avoid closing of the gap by adding the potential $V_\Delta = \Delta \sum_n (c^\dagger_{nA} c_{nA} - c^\dagger_{nB} c_{nB})$, we change the symmetry of the Hamiltonian. The SSH Hamiltonian has inversion symmetry with respect to any mid points between sites A and B. Mathematically the symmetry is implemented by $P_I = \sigma_x \cdot (k \to -k)$. The first factor σ_x interchanges A and B sublattices and the second one changes momentum k to $-k$. It is easy to see that for (6.14)

$$P_I^{-1} \mathcal{H}_{\rm SSH} P_I = \mathcal{H}_{\rm SSH} \tag{6.15}$$

However $V_\Delta = \Delta \sum_{k\alpha\beta} \sigma^z_{\alpha\beta} c^\dagger_{\alpha k} c_{\beta k}$ and $P_I^{-1} V_\Delta P_I = -V_\Delta$. That V_Δ breaks inversion symmetry should also be clear from looking at the picture of the SSH model.

While representation (6.5) that uses $\psi_{A/B,k,\lambda}$ is most convenient for diagonalizing the Hamiltonian, when we discuss topological properties of the Bloch bands and experimental measurements of the Berry/Zak phase, it is better to introduce Bloch functions. As you recall the Bloch functions are defined as $\psi(x) = e^{ikx} u(x)$, where $u(x)$ is periodic. Here x is the actual coordinate and not the position of the center of a unit cell. Thus it is more natural to use $\alpha_{k,\lambda}$ and $\beta_{k,\lambda}$ defined from

$$\psi(x) = e^{ikx} u_k(x) = \sum_n (\alpha_k e^{ik(n-\frac{1}{4})} w_A(x - (n - \frac{1}{4})) + \beta_k e^{ik(n+\frac{1}{4})} w_B(x - (n + \frac{1}{4})) \tag{6.16}$$

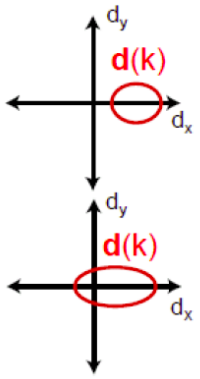

Figure 6.4: Illustartion of the topological character of the SSH Hamiltonian. When $t_2 > t_1$ the vector $d(k)$ goes around the origin. In the opposite case it does not encircle the origin and can be contracted to a point. The two can not be connected smoothly without either going through the origin, which closes the gap between the two bands, or reducing the symmetry of the Hamiltonian.

Here $w_A(x-(n-\frac{1}{4}))$ and $w_B(x-(n+\frac{1}{4}))$ correspond to Wannier functions on the A/B sites in unit cell n. Note also that we chose the origin to be half way between the A and B sites, which respects the inversion symmetry of the model. Hence our Bloch functions $u_{k,\lambda}(x)$ are represented by spinors

$$\begin{pmatrix} \alpha_{k,-} \\ \beta_{k,-} \end{pmatrix} = \frac{1}{\sqrt{2}} \begin{pmatrix} e^{i\frac{k}{4}} \\ e^{-i\frac{3k}{4}-i\theta_k} \end{pmatrix} \qquad \begin{pmatrix} \alpha_{k,+} \\ \beta_{k,+} \end{pmatrix} = \frac{1}{\sqrt{2}} \begin{pmatrix} -e^{i\frac{k}{4}} \\ e^{-i\frac{3k}{4}-i\theta_k} \end{pmatrix} \quad (6.17)$$

We introduce the so-called Berry connection

$$A_\lambda(k) = \frac{1}{i}\langle u_{k,\lambda}|\partial_k u_{k,\lambda}\rangle \quad (6.18)$$

In our case we find

$$A_\pm(k) = -\frac{1}{4} - \frac{1}{2}\frac{d\theta_k}{dk} \quad (6.19)$$

Topological characterization of Bloch bands is conveniently given in terms of the integral of the Berry connection

$$\phi_\pm = \int_{-\pi}^{\pi} dk A_\pm(k) = -\frac{\pi}{2} - sign(t_2 - t_1)\frac{\pi}{2} \quad (6.20)$$

Thus we demonstrated that the Zak phase can only be 0 or π (phase is only defined modulo 2π, so $-\pi$ is the same as π). We can not continuously change between the two cases without either closing the bandgap (i.e. having $t_1 = t_2$) or breaking the inversion symmetry, e.g. by introducing a staggered potential $\Delta\sum_n(c^\dagger_{nA}c_{nA} - c^\dagger_{nB}c_{nB})$. We discussed a specific model, however one can prove a more general statement [2]: in 1d systems with inversion symmetry the Zak phase can be either zero or π.

6.2 Exploring topological properties of Bloch bands with Ramsey/Bloch interference

6.2.1 General formalism of Bloch oscillations

Let us now discuss Bloch oscillations in a dimerized lattice. We consider dynamics of atoms given by the Hamiltonian (see [3, 4] for more details)

$$\mathcal{H} = \mathcal{H}_{\mathrm{SSH}} - F\sum_n((n-\frac{1}{4})c^\dagger_{An}c_{An} + (n+\frac{1}{4})c^\dagger_{Bn}c_{Bn}) \tag{6.21}$$

Now we need to solve Heisenberg equations of motion for the time dependent operator $\hat{\Psi}(t)$

$$\frac{d\hat{\Psi}(t)}{dt} = i[\mathcal{H}, \hat{\Psi}(t)] \tag{6.22}$$

We look for the solution in the form

$$\hat{\Psi}(t) = A(t)\gamma^\dagger_{k_0-vt,-} + B(t)\gamma^\dagger_{k_0-vt,+} \tag{6.23}$$

where $v = F$ is the velocity of Bloch oscillations, and we defined $\gamma^\dagger_{k,\lambda}$ operators previously

$$\gamma^\dagger_{k(t),\lambda} = \frac{1}{\sqrt{2N}}\sum_n(e^{ik(n-\frac{1}{4})}\alpha_{k(t),\lambda}c^\dagger_{nA} + e^{ik(n+\frac{1}{4})}\beta_{k(t),\lambda}c^\dagger_{nB}) \tag{6.24}$$

We have

$$\begin{aligned}\frac{\partial\gamma^\dagger_{k_0-vt,\lambda}}{\partial t} = &-\frac{v}{\sqrt{N}}\sum_n[\,i\alpha_{k,\lambda}(n-\frac{1}{4}) + \frac{\partial\alpha_{k,\lambda}}{\partial t}\,]e^{ik(n-\frac{1}{4})}c^\dagger_{An}\,|_{k=k_0-vt} \\ &-\frac{v}{\sqrt{N}}\sum_n[\,i\beta_{k,\lambda}(n+\frac{1}{4}) + \frac{\partial\beta_{k,\lambda}}{\partial t}\,]e^{ik(n+\frac{1}{4})}c^\dagger_{Bn}\,|_{k=k_0-vt}\end{aligned} \tag{6.25}$$

and

$$[\mathcal{H}, \gamma^\dagger_{k,\lambda}] = \epsilon_{k,\lambda}\gamma^\dagger_{k,\lambda} - \frac{F}{\sqrt{N}}sum_n[\alpha_{k\lambda}e^{ik(n-\frac{1}{4})}c^\dagger_{nA} + \beta_{k\lambda}e^{ik(n+\frac{1}{4})}c^\dagger_{nB}] \tag{6.26}$$

We obtain equations on the coeficients $A(t)$ and $B(t)$

$$-i\dot{A}(t) = \epsilon_{k,-}A - \frac{FA}{i}\langle u_{k_0-vt,-}|\partial_k u_{k_0-vt,-}\rangle - \frac{FB}{i}\langle u_{k_0-vt,-}|\partial_k u_{k_0-vt,+}\rangle \tag{6.27}$$

and a similar equation for B. The last term in equation (6.27) describes non-adiabatic mixing of bands. if we neglect it and take $A(t) = e^{i\phi(t)}$ we obtain

$$\dot{\phi} = \epsilon_{k_0-vt,-} - v\langle u_{k_0-vt,-}|\partial_k u_{k_0-vt,-}\rangle \tag{6.28}$$

The first term is the dynamical phase and the second term is the contribution due to the Berry/Zak phase. We can intgrate this over one period of Bloch oscillations using $vdt = dk$ and find

$$\phi_{\text{Bloch}} = \phi_{\text{dynamical}} + \phi_{\text{Zak}} \tag{6.29}$$

$$\phi_{\text{dynamical}} = \int_0^{T_{\text{B}}} \epsilon_{k(t),\lambda} dt \tag{6.30}$$

$$\phi_{\text{Zak}} = \int_{-\pi}^{\pi} dk \, \langle u_{k_0 - vt,-} | \partial_k u_{k_0 - vt,-} \rangle \tag{6.31}$$

where $T_{\text{B}} = \frac{2\pi}{F}$ is the period of Bloch oscillations.

6.2.2 Experimental protocol

Experimental measurements of the Berry/Zak phase in optical lattices have been done in expriments by Atala et al.[3]. The idea of experiments is to have two hyperfine states that have opposite values of magnetic moments and spin independent optical lattice. In the beginning he condensate is prepared in one of the hyperfine states in the ground state, i.e. at the bottom of the lower band at $k = 0$. Then a $\frac{\pi}{2}$ pulse creates a superposition of the two states. Atoms with the opposite spins begin to move in the opposite direction. After half of the Bloch cycle they reach the same point in the Brillouin zone at quasimomentum $\pm\pi$. Now the second $\frac{\pi}{2}$ pulse converts the relative phase between the two types of atoms into spin polarization that can be measured. The phase difference measured in this Ramsey-like protocol has three contributions

$$\phi_{\text{ramsey}} = \phi_{\text{dynamical}} + \phi_{\text{Zak}} + \phi_{\text{Zeeman}} \tag{6.32}$$

The dynamical phase vanishes because spin up and spin down particles always experience the same values of energy. Getting rid of the Zeeman phase requires either precise control of the magnetic field or doing spin echo type measurements. The group of I. Bloch used the latter and measured the Zak phase of $0.97(2)\pi$ [3].

6.3 Two dimensional systems

6.3.1 Interferometric probes of 2d band topology

Interferometric measurements that we discussed in 1d systems in the previous section can be generalized to 2D systems[4, 5]. Fig. 6.6 shows experimental measurements by the MPQ group of the Berry phase intrgrals in a 2D hexagonal graphene lattice. These experiments verified that loops going around Dirac points of graphene lattice give the integral of the Berry phase of π.

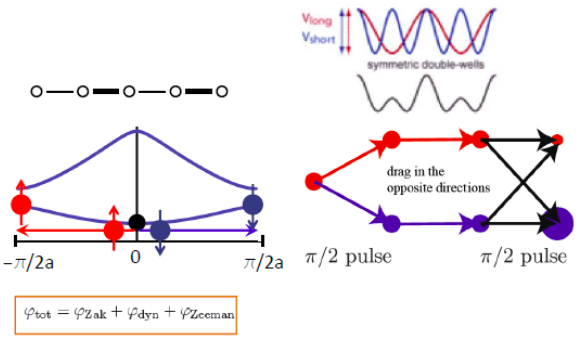

Figure 6.5: Schematic figure of Ramsey/Bloch interference experiments in 1d in [3]. Dimerized potential was created using bichomatic laser beams.

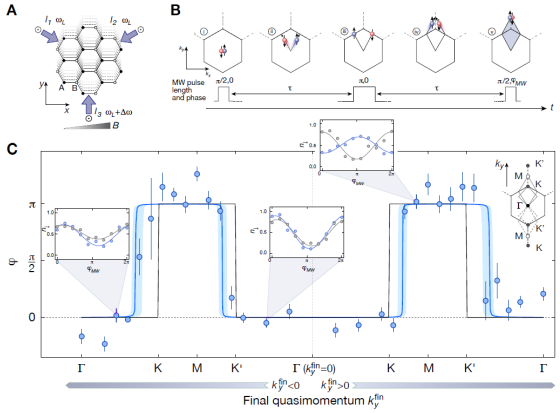

Figure 6.6: Schematic figure of Ramsey/Bloch interference experiments in 2d. Figure from [3]. These experiments demonstrated the π phase when going around the Dirac point of the graphene type lattice.

6.3.2 Anomalous velocity

Consider an atom moving in a 2D Bloch band in the presense of an external force

$$\mathcal{H} = \frac{1}{2m}\left(\frac{\vec{\nabla}}{i}\right)^2 + V(\vec{r}) - \vec{f}\vec{r} \tag{6.33}$$

Here $V(\vec{r}+\vec{a}_i) = V(\vec{r})$ is a periodic lattice potential. First we reduce this problem to the time-dependent Hamiltonian. We look for solutions of the form (recall our discussion of 1d Bloch oscillations)

$$\Psi(r,t) = \tilde{u}(r,t)e^{i\vec{k}(t)\vec{r}} \tag{6.34}$$

$$\vec{k}(t) = \vec{k}_0 + \vec{f}t \tag{6.35}$$

We find

$$i\frac{\partial \tilde{u}}{\partial t} = \frac{1}{2m}\left(\frac{\vec{\nabla}}{i} + \vec{k}(t)\right)^2 \tilde{u} + V(\vec{r})\tilde{u} \tag{6.36}$$

This looks like the usual equation for Bloch wavefunctions but with time-dependent quasimomentum $\vec{k}(t)$. This can be understood as using the gauge $\vec{A} = \vec{E}t$ so that $\frac{\partial \vec{A}}{\partial t} = \vec{E}$. In this gauge the Hamiltonian is translationally invariant hence we can still take $\tilde{u}(r,t)$ to be periodic in the unit cell.

In a generic problem with time-dependent Hamiltonian, in which instantaneous eigenstates are known, and pramaters are being chnaged slowly, we can obtain the leading order correction to adiabatic evolution of the wavefunction. Assume that at time t_0 the wavefunction is given by the instantaneous eigenstate $|\lambda\rangle$. Then at later times

$$|\Psi(t)\rangle = e^{-\int_{t_0}^{t} E_\lambda(t')dt'} \cdot \left\{ |\lambda(t)\rangle - i\sum_{\lambda' \neq \lambda} |\lambda'(t)\rangle \frac{\langle \lambda' | \frac{\partial}{\partial t} | \lambda \rangle}{(E_\lambda - E_{\lambda'})} \right\} \tag{6.37}$$

Note that in (6.37) does not have the Berry phase part. Since we are interested in short time evolution (no closed path trajectories) we absorbed this phase into the redefinition of instantaneous wavefunctions. In the problem (6.35) with Bloch bands and time dependent quasimomentum we find the following non-adiabatic correction to the instantaneous Bloch wavefunctions $|\lambda(t)\rangle$

$$|\tilde{u}_{n,k}(t)\rangle = e^{-i\int_{t_0}^{t} E_{n,k(t')}dt'} \cdot \left\{ |u_{n,k(t)}\rangle - i\sum_{n' \neq n} |u_{n',k(t)}\rangle \frac{\langle u_{n',k(t)} | \frac{\partial}{\partial t} | u_{n,k(t)} \rangle}{(E_{n,k(t)} - E_{n',k(t)})} \right\} \tag{6.38}$$

We now want to calculate the expectation value of the velocity operator $\vec{v}$ in the state $|\tilde{u}_{n,k}(t)\rangle$. Note, that from now on, for brevity I will not write explicitely the time dependence of the evolving $k(t)$, and just use k. For Bloch states u_{nk}

$$\vec{v}_{nk} = \frac{1}{m}\left(\frac{\vec{\nabla}}{i} + \vec{k}\right) = \frac{\partial}{\partial \vec{k}} \mathcal{H}_0(\vec{k}) \tag{6.39}$$

$$\mathcal{H}_0(\vec{k}) = \frac{1}{2m}\left(\frac{\vec{\nabla}}{i} + \vec{k}\right)^2 + V(\vec{r}) \tag{6.40}$$

Taking expectation value of $\vec{v}$ in wavefunction (6.38) we find

$$\tilde{\vec{v}}_{nk} = \frac{\partial \epsilon_n(k)}{\partial \vec{k}} - i\sum_{\lambda = \{n' \neq n, k\}} \left\{ \frac{\langle u_{nk} | \frac{\partial \mathcal{H}_0}{\partial \vec{k}} | u_\lambda \rangle \langle u_\lambda | \frac{\partial u_{nk}}{\partial t} \rangle}{E_{nk} - E_\lambda} - \text{c.c.} \right\} \tag{6.41}$$

With simple manipulations we can transform the last expression into

$$\tilde{\vec{v}}_{nk} = \frac{\partial \epsilon_n(k)}{\partial \vec{k}} - i\sum_{\lambda = \{n' \neq n, k\}} \left\{ \langle \frac{\partial u_{nk}}{\partial \vec{k}} | u_\lambda \rangle \langle u_\lambda | \frac{\partial u_{nk}}{\partial t} \rangle - \text{c.c.} \right\} \tag{6.42}$$

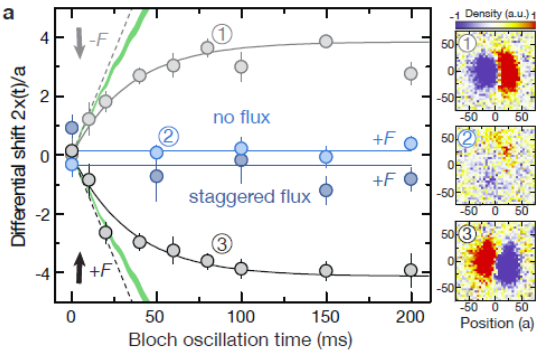

Figure 6.7: Measurements of anomalous velocity in experiments by [8]. Note that band populations are not constant in these experiments, which makes interpretation more difficult. Similar experimental results for a different microscopic Hamiltonian have been reported in [9].

Using

$$|\frac{\partial u_{nk}}{\partial t}\rangle = |\frac{\partial u_{nk}}{\partial \vec{k}}\rangle \vec{f} \tag{6.43}$$

we finally obtain

$$\tilde{\vec{v}}_{nk\alpha} = \frac{\partial \epsilon_n(k)}{\partial k_\alpha} - i\left(\langle \frac{\partial u_{nk}}{\partial k_\alpha} | \frac{\partial u_{nk}}{\partial k_\beta}\rangle - \langle \frac{\partial u_{nk}}{\partial k_\beta} | \frac{\partial u_{nk}}{\partial k_\alpha}\rangle\right) f_\beta \tag{6.44}$$

In the 2D case we can define not only the Berry connection $\vec{A} = \frac{1}{i}\langle u_{nk}|\frac{\partial u_{nk}}{\partial \vec{k}}\rangle$ but also the Berry curvature

$$\vec{\Omega} = \frac{1}{i}\vec{\nabla}_q \langle u_{nq}|\frac{\partial u_{nq}}{\partial \vec{q}}\rangle \tag{6.45}$$

$$\Omega_{\alpha\beta} = \frac{1}{i}\left(\langle \frac{\partial u_{nk}}{\partial k_\alpha} | \frac{\partial u_{nk}}{\partial k_\beta}\rangle - \langle \frac{\partial u_{nk}}{\partial k_\beta} | \frac{\partial u_{nk}}{\partial k_\alpha}\rangle\right) \tag{6.46}$$

Thus our analysis can be summarized in a very simple formula

$$\vec{v}_{nk} = \frac{\partial \epsilon_n(k)}{\partial \vec{k}} + \vec{f} \times \vec{\Omega} \tag{6.47}$$

For a more detialed discussion of anomolous velocity, see [6, 7, 8, 9].

In the next section we will prove that the integral of the Berry curvature over the entire 2D Brillouin zone is quantized. This is the celebrated Chern number responsible for the quantization of the Hall conductance in 2-dimensional electrons. For a more detailed discussion of topological states in traditional solid state systems see Refs. [6, 10, 11]

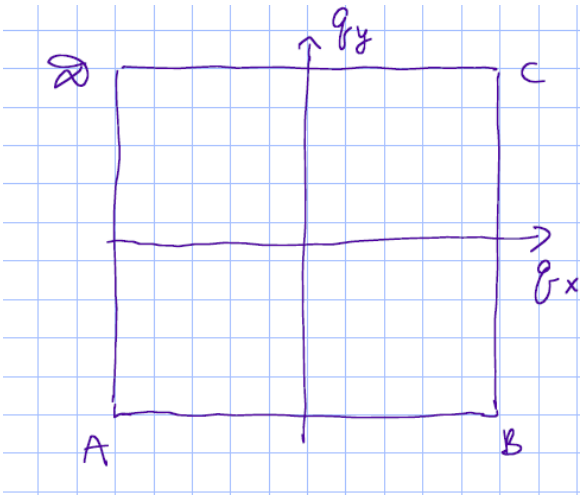

Figure 6.8: We introduce 4 points at the corners of the Brillouin zone A=(-π,-π), B=(π,-π), C=(π,π), D=(-π,π).

6.3.3 Chern number

Integral of the Berry curvature over a 2D Bloch band is called the Chern number. It is quantized in units of 2π as we demonstrate below.

For simplicty we assume that the Brillouin zone has the shape of a square, see fig. 6.8. This is not important for the proof, but simplifies the argument. A more accurate discussion can be found in [12]. Let us consider the integral

$$I = \int_{\mathrm{BZ}} d^2q\, \Omega_{xy} \tag{6.48}$$

with

$$\Omega_{xy} = \frac{\partial A_x}{\partial q_y} - \frac{\partial A_y}{\partial q_x} \tag{6.49}$$

$$A_\alpha = \frac{1}{i}\langle u_q | \frac{\partial}{\partial q_\alpha} u_q \rangle \tag{6.50}$$

By Stokes theorem we have

$$I = \oint_{A\to B\to C\to D\to A} d\vec{q}\vec{A}(q) \tag{6.51}$$

$$= \int_A^B dq_x A_x(q_x,-\pi) + \int_B^C dq_y A_y(\pi,q_y) + \int_C^D dq_x A_x(q_x,\pi) + \int_D^A dq_y A_y(-\pi,q_y)$$

$$= \int_{-\pi}^{\pi} dq_x (A_x(q_x,-\pi) - A_x(q_x,\pi)) + \int_{-\pi}^{\pi} dq_y (A_y(\pi,q_y) - A_y(-\pi,q_y)) \tag{6.52}$$

We assume that we have Bloch functions everywhere in the Brilluin zone $|u(q)\rangle$. Since points $(q_x, \pm\pi)$ are physically the same, Bloch states at these points can

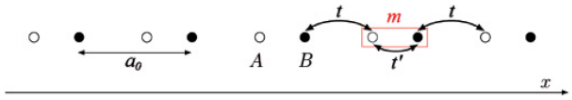

Figure 6.9: Figure for problem 1. Finite chain.

only differ in the overall phase. Analogous arguments works for points $(\pm\pi, q_y)$. Thus we should have

$$|u(q_x,\pi)\rangle = e^{i\theta_x(q_x)}|u(q_x,-\pi)\rangle \tag{6.53}$$
$$|u(\pi,q_y)\rangle = e^{i\theta_y(q_y)}|u(-\pi,q_y)\rangle \tag{6.54}$$

This leads to the following relations

$$A_x(q_x,\pi) = -\partial_x\theta_x(q_x) + A_x(q_x,-\pi) \tag{6.55}$$
$$A_y(\pi,q_y) = -\partial_y\theta_y(q_y) + A_y(-\pi,q_y) \tag{6.56}$$

We can use these relations to rewrite (6.52) as

$$\begin{aligned} I &= \int_{-\pi}^{\pi} dq_x \partial_x\theta_x(q_x) - \int_{-\pi}^{\pi} dq_y \partial_y\theta_y(q_y) \\ &= \theta_x(\pi) - \theta_x(-\pi) - \theta_y(\pi) + \theta_y(-\pi) \end{aligned} \tag{6.57}$$

From the matching relations at the corners we have

$$|u_{\rm B}\rangle = e^{i\theta_y(-\pi)}|u_{\rm A}\rangle \tag{6.58}$$
$$|u_{\rm C}\rangle = e^{i\theta_x(\pi)}|u_{\rm B}\rangle \tag{6.59}$$
$$|u_{\rm D}\rangle = e^{-i\theta_y(\pi)}|u_{\rm C}\rangle \tag{6.60}$$
$$|u_{\rm A}\rangle = e^{-i\theta_x(-\pi)}|u_{\rm D}\rangle \tag{6.61}$$

Then

$$|u_{\rm A}\rangle = e^{i\theta_y(-\pi)+i\theta_x(\pi)-i\theta_y(\pi)-i\theta_x(-\pi)}|u_{\rm A}\rangle \tag{6.62}$$

which requires

$$\theta_y(-\pi) + \theta_x(\pi) - \theta_y(\pi) - \theta_x(-\pi) = 2\pi n \tag{6.63}$$

From (6.57) and (6.63) we find that

$$\int_{\rm BZ} d^2q\, \Omega_{xy} = 2\pi n \tag{6.64}$$

6.4 Problems for Chapter 6

Problem 1 Solve single particle spectrum for a finite chain as shown in fig. 6.9. Pay special attention to the possibility of localized states at the edges. Discuss the relation between the existence of edge states and topological character of the Zak phase of the corresponding bulk Hamiltonian.

Bibliography

[1] A.J. Heeger, S A Kivelson, J.R. Schrieffer, and W.-P. Su. Solitons in conducting polymers. *Rev. Mod. Phys.*, 60:783, 1988.

[2] J Zak. Berry ' s Phase for Energy Bands in Solids given the adiabatic form. *Physical Review*, 62(23):2747–2750, 1989.

[3] Marcos Atala, Monika Aidelsburger, Julio T. Barreiro, Dmitry Abanin, Takuya Kitagawa, Eugene Demler, and Immanuel Bloch. Direct measurement of the Zak phase in topological Bloch bands. *Nature Physics*, 9(12):795–800, November 2013.

[4] Dmitry Abanin, Takuya Kitagawa, Immanuel Bloch, and Eugene Demler. Interferometric Approach to Measuring Band Topology in 2D Optical Lattices. *Physical Review Letters*, 110(16):165304, April 2013.

[5] L Duca, T Li, M Reitter, I Bloch, and U Schneider. An Aharonov-Bohm interferometer for determining Bloch band topology. *arXiv:1407.5635*.

[6] Di Xiao, Ming-che Chang, and Qian Niu. Berry Phase Effects on Electronic Properties. *Reviews of Modern Physics*, 82:1959, 2010.

[7] H. M. Price and N. R. Cooper. Mapping the Berry curvature from semiclassical dynamics in optical lattices. *Physical Review A*, 85(3):033620, March 2012.

[8] M Aidelsburger, M Lohse, C Schweizer, M Atala, J T Barreiro, N R Cooper, I Bloch, and N Goldman. Revealing the topology of Hofstadter bands with ultracold bosonic atoms. *arXiv:1407.4205*, pages 1–18.

[9] Gregor Jotzu, Michael Messer, Martin Lebrat, Thomas Uehlinger, Daniel Greif, and Tilman Esslinger. Experimental realisation of the topological Haldane model. *arXiv:1406.7874*, 2014.

[10] Xiao-Liang Qi and Shou-Cheng Zhang. Topological insulators and superconductors. *Reviews of Modern Physics*, 83(4):1057–1110, October 2011.

[11] M. Hasan and C. Kane. Colloquium: Topological insulators. *Reviews of Modern Physics*, 82(4):3045–3067, November 2010.

[12] Mahito Kohmoto. Topological invariant and the quantization of the Hall conductance. *Annals of Physics*, 160(2):343–354, April 1985.